Surf Interface Anal. 2017;1‐8. DOI: 10.1002/sia.6260

Exploiting carbon-based (Cr,Ce)/a-C:H nanocomposite film on cemented WC

Shengguo Zhou[1], Zhengbing Liu[1], Shuncai Wang[2]

[1] School of Material Science and Engineering, Jiangxi University of Science and Technology, Ganzhou, Jiangxi 341000, China
[2] National Centre for Advanced Tribology at Southampton (nCATS), School of Engineering Sciences, University of Southampton, Southampton SO17 1BJ, UK
[1] Correspondence: Shengguo Zhou, Email: zhousg@jxust.edu.cn

Cemented tungsten carbide (WC) has widely served in modern industry because of its outstanding characteristics, while it could suffer from severely wear both under ambient air and water environments. To exploit a novel carbon-based film should be a feasible way to modify the surface of cemented WC and overcome these shortcomings. In the present study, the Cr/Ce co‐incorporated (Cr,Ce)/a-C:H carbon-based film was successfully deposited on cemented WC. The microstructure and mechanical properties of films were systematically characterized, and their tribological behaviors were tested in ambient air and deionized water environment. The results showed that (Cr,Ce)/a-C:H film dominated by the typical amorphous structure and the doping Cr existed with the metallic Cr nanocrystallites as well as Ce formed CeO2. The (Cr,Ce)/a-C:H film could possess good mechanical performances, which could own higher hardness, elastic module, low internal stress, and better adhesive strength. Especially, the as-prepared (Cr,Ce)/a-C:H film could present relatively lower friction coefficient and wear rate compared to uncoated cemented WC both under ambient air and deionized water environment, indicating that the Cr/Ce co‐doped (Cr,Ce)/a-C:H film could be an effective method to modify the surface of cemented WC so as to improve the friction and wear performances of cemented WC materials.

KEYWORDS: (Cr,Ce)/a-C:H, tribological behaviors, cemented WC

1 INTRODUCTION

Because of outstanding chemical and superior mechanical characteristics, cemented tungsten carbide (WC) has been used for metal cutting ever since its very first invention.[1] Moreover, the researchers could prepare a novel cemented WC that achieved a dramatically increased combination of hardness, wear resistance, fracture toughness, and strength as a result of precipitation of extremely fine nanoparticles in the cobalt binder of cemented carbides, and then this kind of novel cemented carbide could have better antiwear performances.[2,3] However, cutting inserts have to endure high mechanical and thermal loads during application. To cope with this problem, cutting water-based fluid is applied to reduce the cutting temperature and also to provide lubrication, which can improve tool life to some extent. Consequently, the lifetime of cemented WC could be improved within cutting water based fluid while its wear is still severe.[1,4] To cope with the challenge, modified the surface of cemented WC with a low-friction and wear resisting film, such as TiN, TiCN, and diamond-like carbon (DLC), should be a valid method. Compared to TiN and TiCN, DLC could have better tribological performances.[5,6]

The investigation for DLC, a new function material, has attracted much attention for their important applications in the fields of solid state devices and self-lubrication, because of their exceptional properties, such as low-friction characteristics, low wear, high hardness, and high elastic modulus, as well as chemical inertness, in recent years.[7-10] Numerous research reports that DLC films have a tendency to show poor adhesion to various substrates and even causes the peeling of films from the substrates owing to the high internal stress, which up to 10 GPa in DLC films, and will limit the deposition thickness and field of applications.[7,11,12] The incorporation of other metallic elements (like Cr, Ti, or W) into the DLC (Me-DLC) films and metallic transition layer provides an effective way to improve their internal stress and adhesion strength to the substrate, respectively.[7,8,13,14] The Me-DLC films form the nanocrystallines that are dispersed in

the DLC amorphous structure. The change of microstructure of the DLC films generally accompanies the distortion of bond angles of tetrahedral bonds and sp3 bonds, leading to degrade hardness and elastic modulus and improve internal stress and adhesion strength.[12,13] Moreover, the effect on microstructure and performance of trace rare earth elements doping in DLC films has been reported, and DLC films could exhibit good tribological properties.[15] It is reported that rare earth element is doped into DLC films where it would be dissolved within the DLC amorphous matrix but not formed nanocrystallines.[15-17] Therefore, co-doping rare earth element Ce into Me-DLC films may also have a positive effect on the friction-reduction and antiwear properties on the surface of cemented WC. Although some reports have discussed the structure and mechanical properties of Cr-DLC films or rare earth element modified DLC films, the rare earth element Ce accompanied by metallic Cr to prepare duplex doped nanocomposite carbon-based film is seldom reported. In addition, this rare earth Ce-modified carbon-based film as a strategy to improve tribological performances of cemented WC is seldom reported.

In present study, the selected rare earth Ce and metal Cr were codoped in DLC to prepare novel (Cr,Ce)/a-C:H carbon-based film so as to improve cemented WC. The morphologies, microstructure, and mechanical properties of as-deposited (Cr,Ce)/a-C:H carbon-based film were investigated systematically, and the friction and wear behaviors were evaluated both in ambient air and in deionized water conditions. It would expect that the as-prepared (Cr,Ce)/a-C:H carbon-based film can be used to improve tribological performances of cemented WC both in ambient air and the water environments.

2 EXPERIMENTAL

2.1 Deposition method

The hydrogenated (Cr,Ce)/a-C:H carbon-based film was deposited on Si p(100) wafers and cemented WC (Co% = 8 at%) substrates by using a DC reactive magnetron sputtering system. CementedWC substrates were prepared with mirror polished, and the sizes of specimens were 30 mm × 30 mm × 2 mm. Herein, solitary Cr-doped Cr/a-C:H was prepared simultaneously so as to compare with (Cr,Ce)/a-C:H film. Because Co phase can induce interfacial graphitization and cause the adhesion deteriorated,[18] so a pretreatment process was implemented to remove the Co phase from cemented WC substrate surface: Cemented WC substrates were ultrasonically cleaned in the acetone (20 min), ethanol (20 min), deionized water (10 min), potassium hydroxide solution (10 g KOH + 100 mL H2O) (30 min), Caro's acid (30 mL H2SO4:70 mL H2O2) (1 min), and deionized water (10 min) in succession and dried in nitrogen blow as follows. Prior to deposition, the base pressure of vacuum chamber must be evacuated 2.0 × 10−3 Pa. When the base pressure of the vacuum chamber was reached, the metallic Cr interlayer was deposited so as to improve adhesion strength of the substrates and carbon-based film by using 2 Cr targets (purity > 99.99 wt%). The deposition parameters of Cr interlayer were described as follows: deposition pressure of 3.0 Pa, Ar flow rate of 60 sccm, a Cr target sputtering power of 200 W, deposition temperature of 200°C, and deposition time of 15 minutes. Carbon-based films were deposited by using 2 targets in CH4 and Ar mixing gas atmosphere on top of the Cr interlayer. Two Cr targets were used for Cr/ a-C:H films, while one Cr target and one Cr/Ce composite target (Cr concentration of 90 at%) were used for (Cr,Ce)/a-C:H film. The deposition parameters of top films were shown as follows: pressure of 2.0 Pa, Ar flow rate of 50 sccm, sputtering power of 160 W, temperature of 100°C, deposition time of 90 minutes, and the CH4 flow rate for Cr/a-C:H film was 10 sccm, for (Cr,Ce)/a-C:H film was 14 sccm.

2.2 Measuring methods

The microstructure of the Cr/a-C:H and (Cr,Ce)/a-C:H films was characterized by X-ray photoelectron spectroscopy (XPS), X-ray diffraction (XRD), and transmission electron microscope. The final thickness and root mean square (RMS) roughness were evaluated by field emission scanning electron microscope (FESEM) and atomic force microscopy (AFM). The hardness and adhesion strength were evaluated using MTS Nano-indenter system and Revetest CSM scratch tester. The friction and wear behaviors of the Cr/a-C:H and (Cr,Ce)/a-C:H films were evaluated on the UMT-3 reciprocating sliding tribometer both in ambient air condition and deionized water condition at room temperature. The cemented WC ball with a diameter of 6 mm was used as the counter body, and all frictional tests were performed under a load of 5 N with the amplitude of 5 mm and reciprocating frequency of 5 Hz. As follow, the morphologies of the wear tracks and wear scars were characterized using a scanning electron microscope (SEM). Meanwhile, the wear rates calculated after the sliding tests were completed basing on the wear track depth profiles detected by a NanoMap 500LS profilometer.

3 RESULTS AND DISCUSSION

3.1 Characteristics of as-prepared carbon-based films

X-ray photoelectron spectroscopy was used to characterize the Cr/a- C:H and (Cr,Ce)/a-C:H carbon-based films, and Figure 1 shows the high-resolution C1s and Ce3d spectra and the chemical composition. Thus, the composition of as-prepared films could be detected that it was about 97.5 at% C and 0.8 at% Cr for solitary Cr/a-C:H film and it was about 94.0 at% C, 0.9 at% Cr, and 0.3 at% Ce for duplex doped (Cr,Ce)/a-C:H film. In addition, the chemical state of atoms could be analyzed by XPS fine spectrum. The Ce3d XPS spectra, as shown in Figure 1A, showed the 3d5/2 and 3d3/2 transitions at the binding energy of 881.7 and 900 eV that the distance was about 18.3 eV and the spectrum exhibited 2 associated satellite peaks at the binding energy of 904.3 and 885.8 eV. Therefore, it could confirm that the Ce existed in the form of metal oxide.[15,16] Furthermore, the XPS C1s spectrum of the Cr/a-C:H and (Cr,Ce)/a-C:H carbon-based films, as shown in Figure 1B, was deconvoluted into 3 Gaussian lines centered at 284.5, 285.4, and 286.9 eV corresponding to the sp2, sp3, and C–O bonds, respectively, whereas there were no Cr–C bonds according to characteristic the XPS C1s spectrum. Besides, the value of sp3/ (sp2 + sp3) could be calculated through the deconvoluted peak intensity; so the relative content of sp3 bond was about 0.23 for the Cr/a- C:H film while it was about 0.25 for the (Cr,Ce)/a-C:H film. It was reported that sp3 content could increase with the increase of CeO2 content when the CeO2 content was ≤4 at%.[15]

X-ray diffraction was used to analyze the phase in as-prepared Cr/a-C:H and (Cr,Ce)/a-C:H films, and the corresponding spectrum was depicted in Figure 2. It could be observed that both the XRD spectra of as-prepared films showed a similar diffraction peak except for the intensity. The diffraction peak in the XRD spectrum corresponded to the (110) and (211) planes of Cr. Thus, there was only Cr crystal peak excluding that of silicon substrate while there was no any information about Ce or CeO2. The intensity of (211) diffraction peak was decreased obviously as the co-doping with rare earth Ce. As we known, the value of full width at half maximum of diffraction peak was affinitive to the crystallinity of the Cr phase, so it could investigate the growth of Cr grains in the films by the full width at half maximum of the peaks of Cr phase. According to Debye-Scherrer's formula,19 it could calculate that the average crystalline size of Cr was about 7 nm for Cr/a-C:H film and 5 nm for (Cr,Ce)/a-C:H film. As a result, Ce co-doping could restrain the crystallinity of the Cr phase in the film.

To further detect the microstructure of as-prepared carbon-based films, HRTEM was conducted to identify their nanocrystalline and amorphous characteristic. Figure 3 illustrates the High-resolution transmission electron microscope

(HRTEM) bright-field images of as-prepared Cr/a-C:H and (Cr,Ce)/a-C:H carbon-based films. As we seen, both of Cr/a-C:H and (Cr,Ce)/a-C:H carbon-based films had typical nanocrystallites/amorphous microstructure where the nanoparticles (black dots in the images) were uniformly embedded in the amorphous carbon matrix (bright area in the images). The corresponding size of grains was about 7 nm for the Cr/a-C:H and about 5 nm for (Cr,Ce)/a-C:H carbon-based films. Previous studies reported that the metallic Cr mainly existed in 2 forms in the DLC: One was Cr atoms could form nanocrystals (CrxCy) by bonding with C atoms in the carbon matrix, and the other was Cr atoms could melt in carbon matrix in terms of atoms or atomic clusters.[20] And it was reported that as the Cr concentration is ≤1.8 at%, CrxCy was not generated by reaction between C and Cr.[21] As analyzed by previous XPS and XRD, the nanoparticles could be recognized to metallic Cr phase. Besides, all the Ce dopant was dissolved within the DLC amorphous matrix existed with CeO2 when the CeO2 content was ≤8 at%.[22] As a result, the co-doped (Cr,Ce)/a-C:H carbon-based film could present the microstructure mainly consisted of Cr nanocrystallites and amorphous carbon as well as dissolved CeO2.

Figure 4 shows the 3-dimensional AFM surface morphologies of as-prepared 2 kinds of Cr/a-C:H and (Cr,Ce)/a-C:H films. It can be seen that the surfaces were mainly consisted of nanoscale concave-convex body, where the sizes were about 100 to 200 nm. The RMS roughness was calculated that it was about 2.28 nm for Cr/a-C:H film and 1.03 nm for (Cr,Ce)/a-C:H film. The result showed the surface morphologies were little difference between Cr/a-C:H and (Cr,Ce)/a-C:H carbon-based films.

Besides, the cross section of Cr/a-C:H and (Cr,Ce)/a-C:H films characterized by FESEM was shown in Figure 5. As seen in the images of FESEM, there was a small difference in the thickness that was about 1.05 μm for Cr/a-C:H film and 1.16 μm for (Cr,Ce)/a-C:H film. The small difference should be attributed that the rare earth Ce atoms were easier sputtered and ionized so that the sputtered Ce atoms had the more possibility to deposit on the substrate if the same sputtering power of targets causing the same electric field between the target and substrate.[23] The cross-sectional morphologies presented typical columnar structure for Cr/a-C:H film while the columnar was weaken for (Cr,Ce)/a-C:H film. In particular, the interfaces did not suffer from any visibly localized delamination indicating a good adhesion of as-prepared films to the substrate. Bedsides, the rare earth Ce co-doped (Cr,Ce)/a-C:H film could have more dense and homogeneous structure compared to Cr-doped Cr/a-C:H film.

3.2 Mechanical properties

The hardness (H), elastic modulus (E), H/E ratio extracted from nanoindentation of as-prepared carbon-based films were presented in Figure 6. The hardness and elastic modulus of (Cr,Ce)/a-C:H film showed an increased value compared to Cr/a-C:H film. The hardness (H) was an essential constant and equal to 18.6 GPa for Cr/a-C:H film and 22.0 GPa for (Cr,Ce)/a-C:H film. The elastic modulus (E) also exhibited an increase from 144.1 GPa for Cr/a-C:H film to 169.6 GPa for (Cr,Ce)/a-C:H film. The value of the H/E ratio of both carbon-based films was nearly 0.13, which indicated the wear rate of these 2 carbon-based films should be very close.[24] As analyzed by above XPS, there was a relatively higher content of sp3 in (Cr,Ce)/a-C:H film so that it should have higher hardness compared to the Cr/a-C:H film. Besides, CeO2 was the main component of glass-polishing materials that should own high hardness, indicating that the Ce modified (Cr,Ce)/a-C:H carbon-based film could possess higher hardness.[25]

Also, the internal stress of the as-prepared films was tested. The value of internal stress equaled to 2.01 GPa for Cr/a-C:H film and 1.22 GPa for (Cr,Ce)/a-C:H film and showed Ce resulted in a significant influence. During the CeO2 dissolved within the amorphous matrix process, the doped Ce atom could play the more roles as a pivotal site, where distortion of the atomic bond angles could occur without inducing a significant increase in the elastic energy, indicating that it could effectively reduce the internal stress within the carbon-based films.[26] Dissolved CeO2 played an important role in the improvement of internal stress. Besides, the adhesive strength of as-prepared films was evaluated, and the optical microscope images and acoustic emission (AE) of scratch tracks were shown in Figure 7. It can be seen that Cr/Ce co-doped (Cr,Ce)/a-C:H film had an increase of critical load to 37 N while the solitary Cr/a-C:H film just had a critical load of 23 N from scratch images and AE. Obviously, the as-prepared films both presented intense acoustic emission (AE) at critical load. In addition, it could found more cracks and abruptly localized delamination of severely brittle characteristic on the scratch track for Cr/a-C:H film while it mainly presented plastically deformation and some microcracks for the (Cr,Ce)/a-C:H film. The CeO2 dissolved within the DLC amorphous matrix and not formed nanoparticles decreased internal stress and improve adhesive strength. As a result, it could achieve a much more high adhesive strength compared to Cr/a-C:H film. Therefore, Cr/Ce co-doped in DLC should be a good way to enhance carbon-based films so that (Cr,Ce)/a-C:H film could have relatively good combined mechanical properties.

3.3 Tribological performances

The tribological performances of cemented WC substrate, Cr/a-C:H, and (Cr,Ce)/a-C:H films were tested in ambient air condition, as shown in Figure 8. The wear tracks were detected by profilometer, and their corresponding wear rates were calculated. The results showed that the friction coefficient could get a stable value of 0.17 for the Cr/a-C:H film and 0.13 for the (Cr,Ce)/a-C:H film, while the friction coefficient for cemented WC substrate was always a high value and fluctuated obviously. And the wear rate was 6.8 × 10−7 mm3/(Nm) for cemented WC substrate, 2.74 × 10−7 mm3/(Nm) for the Cr/−C:H film, and 1.32 × 10−7 mm3/(Nm) for the (Cr,Ce)/a-C:H film. Furthermore, the morphologies of wear tracks and their corresponding wear scars were characterized by SEM, as shown in Figure 9. It can be seen that cemented WC owned the most severe wear, while (Cr,Ce)/a-C:H film presented slighter wear compare to Cr/a-C:H film. Therefore, the as-prepared films presented excellent protecting effect for the cemented WC.

At the same time, the tribological performances of cemented WC substrate, Cr/a-C:H, and (Cr,Ce)/a-C:H films were tested under the deionized water condition, as shown in Figure 10. The (Cr,Ce)/a-C:H film presented relatively lower friction coefficient and wear rate under the deionized water to Cr/a-C:H film. It could be seen that the friction coefficient reached a stable value of 0.11 for the Cr/a-C:H film and 0.07 for the (Cr,Ce)/a-C:H film, while the friction coefficient of cemented WC substrate fluctuated from 0.23 to 0.28 in about every 7 seconds. And the wear rate was 3.8 × 10−7 mm3/(Nm) for cemented WC, 1.82 × 10−7 mm3/(Nm) for Cr/−C:H film, and 8.2 × 10−8 mm3/(Nm) for the (Cr,Ce)/a-C:H film. Also, the morphologies of wear tracks and wear scars were characterized by SEM, as shown in Figure 11. The (Cr,Ce)/a-C:H films showed slight wear merely. Obviously, the wear scar diameter of cemented WC was relatively large, and the (Cr,Ce)/a-C:H film presented smaller wear scar diameter compared to Cr/a-C:H film. There were some granular chips on the ball surfaces of the as-prepared carbon-based films.

3.4 Discussion

The as-prepared carbon-based films exhibited low-friction coefficients and wear rate compared to uncoated cemented WC both in ambient air and in deionized water condition. Especially, (Cr,Ce)/a-C:H film presented lower friction coefficient and wear rate than Cr/a-C:H film in ambient air condition. High hardness would prevent from wear due to high carrying capacity under the action of high-speed friction testing. As a result, lower RMS, the relatively high content of sp3 fraction, and hardness were important factors to the low-friction coefficient and wear rate for the (Cr,Ce)/a-C:H film compared to Cr/a-C:H film in ambient air condition.[24,27-29] As analyzed by above XPS, AFM, and mechanical properties, (Cr,Ce)/a-C:H film owned relatively higher content of sp3 fraction, lower RMS, and higher hardness compared to Cr/a-C:H film. Besides, numerous reports on tribological behaviors of DLC film confirmed that the low-friction should have a connection to graphitization at asperity contact area. Thus, low shear strength would form between the ball and the film and lead to a low friction coefficient, as shown in SEM images of wear scars. In addition, CeO2 could act as a catalyst to accelerate physicochemical reactions, and then it would cause the enrichment of C and O elements to the friction surface.[30] Therefore, it can be inferred that CeO2 in the (Cr,Ce)/a-C:H film could facilitate the formation of the graphitic transferred layer and enhance the tribological ability of carbon-based film in ambient air condition.

Similarly, uncoated cemented WC was still severe wear, and the as-prepared hydrogenated carbon-based films exhibited slight wear merely as the frictional tests were under deionized water. And all the wear rate of uncoated cemented WC and as-prepared hydrogenated carbon-based films tested under deionized water decreased. The deionized water could provide lubrication and carry off quantity of heat as the uncoated cemented WC was tested. However, the result was contrary to the previous reports. The research result of Ali Erdemir showed that a-C:H film was sensitive to water molecules and the a-C:H film could be severe wear in water environment. [31] Ronkainen et al investigated the tribological properties of a range of hydrogenated DLC films in ambient air and deionized water condition, and results showed hydrogenated DLC films presented higher wear rate in deionized water.[32] However, the roughness of hydrogenated DLC films that had been reported was about 0.01 to 0.03 μm or did not illustrate.[31-33] When hydrogenated carbon-based films friction tested in deionized water, the higher roughness might contribute to the formation of micro-cracks, and water molecules would penetrate into films along the micro-cracks, indicating that the wear rate would be serious. Therefore, the lower roughness might be an important factor for lower wear rate as the hydrogenated carbon-based film was tested in water condition. The as-prepared hydrogenated carbon-based films owned relatively lower roughness to result in low-friction coefficient and wear rate in deionized water. Besides, high hardness and elastic modulus would be effective to restrain wear. Therefore, the (Cr,Ce)/a-C:H film presented lower friction coefficient and wear rate than that of Cr/a-C:H film. As a result, the selected rare earth Ce and metal Cr co-doped (Cr,Ce)/a-C:H film could be feasible to improve tribological performances of cemented WC both in ambient air and the water environments.

4 CONCLUSIONS

The as-prepared carbon-based films exhibited lower friction coefficient and wear rate compared to uncoated cemented WC both in ambient air and in deionized water condition, which could improve the tribological properties of cemented WC significantly. The results could be summarized as follows:

1. The relatively content of doping Cr was about 0.9 at% existed with Cr nanocrystallites and uniformly dispersed in the amorphous carbon matrix, while the doping Ce relatively content was about 0.3 at% and could form CeO2 existed with amorphous phase for the co-doped (Cr,Ce)/a-C:H carbon-based film.

2. The wear test in ambient air showed that the (Cr,Ce)/a-C:H carbon-based film exhibited lower wear rate 1.32 × 10−7 mm3/(Nm) that was less than 51.8% of the Cr/a-C:H film and 80.6% of the cemented WC.

3. As it was in the deionized water, the wear rate of (Cr,Ce)/a-C:H film was 8.2 × 10−8 m3/(Nm) that was less than 54.9% of the Cr/a-C:H film and 78.4% of the cemented WC, indicating that this kind of novel (Cr,Ce)/a-C:H film could be feasible to improve tribological performances of cemented WC.

ACKNOWLEDGEMENTS

This work is supported by the National Natural Science Foundation of China (grant nos 51365016 and 51611130190) and Program for Excellent Young Talents, JXUST.

REFERENCES

1. Chen J, Liu W, Deng X, Wu S. Tool life and wear mechanism of WC–5TiC–0.5VC–8Co cemented carbides inserts when machining HT250 gray cast iron. Ceram Int. 2016;42:10037-10044.
2. Konyashin IY, Ries B, Lachmann F, Mazilkin AA, Straumal BB. Novel hardmetal with nano-strengthened binder. Inorganic Materials: Applied Research. 2011;2:19-21.
3. Konyashin I, Lachmann F, Ries B, et al. Strengthening zones in the co matrix of WC–co cemented carbides. Scr Mater. 2014;83:17-20.
4. Li X, Liu Y, Liu B, Zhou J. Effects of submicron WC addition on structures, kinetics and mechanical properties of functionally graded cemented carbides with coarse grains. Int J Refract Met Hard Mater. 2016;56:132-138.
5. Ng C, Chan O, Man H. Formation of TiN grid on NiTi by laser gas nitriding for improving wear resistance in Hanks' solution. Journal of Materials Science & Technology. 2016;32:459-464.
6. Wang Q, Zhou F, Gao S, Zhou Z, Li LK-Y, Yan J. Effect of counterparts on the tribological properties of TiCN coatings with low carbon concentration in water lubrication. Wear. 2015;328-329:356-362.
7. Yang W, Guo Y, Xu D, et al. Microstructure and properties of (Cr:N)-DLC films deposited by a hybrid beam technique. Surface & Coatings Technology. 2014;261:398-403.
8. Kvasnica S, Schalko J, Eisenmenger-Sittner C, et al. Nanotribological study of PECVD DLC and reactively sputtered Ti containing carbon films. Diamond Relat Mater. 2006;15:1743-1752.
9. Shaha KP, Pei YT, Martinez-Martinez D, Sanchez-Lopez JC, Hosson JTMD. Effect of process parameters on mechanical and tribological performance of pulsed-DC sputtered TiC/a-C:H nanocomposite films. Surface & Coatings Technology. 2010;205:2633-2642.
10. Wang F, Wu W, Li J, Li S, Tang Y, Sun W. Extraordinary self-lubrication properties of non-hydrogenated diamond-like carbon films under humid atmosphere. Science in China Series E: Technological Sciences. 2008;52:850-856.
11. Zhang S, Xuan LB, Fu Y. Magnetron-sputtered nc-TiC/a-C(Al) tough nanocomposite coatings. Thin Solid Films. 2004;6035:261-266.
12. Pu J, Zhang G, Wan S, Zhang R. Synthesis and characterization of low friction Al-DLC films with high hardness and low stress. Journal of Composite Materials. 2015;49:199-207.
13. Zou CW, Wang HJ, Feng L, Xue SW. Effects of Cr concentrations on the microstructure, hardness, and temperature-dependent tribological properties of Cr-DLC coatings. Appl Surf Sci. 2013;286:137-141.
14. Qiang L, Gao K, Zhang L, Wang J, Zhang B, Zhang J. Further improving the mechanical and tribological properties of low content Ti-doped DLC film by W incorporating. Appl Surf Sci. 2015;353:522-529.
15. Zhang Z, Jia Z, Wang Y, Wang F, Yang R. Microstructure and characterization of La2O3 and CeO2 doped diamond-like carbon nanofilms. Surf Coat Technol. 2008;202:5947-5952.
16. Zhang Z, Zhou H, Guo D, Gao H, Kang R. Optical characterization of hydrogen-free CeO2 doped DLC films deposited by unbalanced magnetron sputtering. Appl Surf Sci. 2008;255:2655-2659.
17. Zhang Z, Lu X, Luo J, Liu Y, Zhang C. Preparation and characterization of La 2 O 3 doped diamond-like carbon nanofilms (I): structure analysis. Diamond & Related Materials. 2007;16:1905-1911.
18. Zhang D, Shen B, Sun F. Study on tribological behavior and cutting performance of CVD diamond and DLC films on co-cemented tungsten carbide substrates. Appl Surf Sci. 2010;256:2479-2489.
19. Zdujić MV, Milošević OB, Karanović LČ. Mechanochemical treatment of ZnO and Al2O3 powders by ball milling. Mater Lett. 1992;13:125-129.
20. Zhuang Y, Jiang X, Rogachev AV, et al. Influences of pulse frequency on the structure and anti-corrosion properties of the a-C:Cr films. Appl Surf Sci. 2015;351:1197-1203.
21. Jelinek M, Zemek J, Vandrovcova M, et al. Bonding and bio-properties of hybrid laser/magnetron Cr-enriched DLC layers. Mater Sci Eng C Mater Biol Appl. 2016;58:1217-1224.

22. Zhang Z, Lu X, Guo D, Xu J, Luo J. Microstructure and mechanical properties of CeO2 doped diamond-like carbon films. Diamond Relat Mater. 2008;17:396-404.
23. Zhang Z, Lu X, Luo J, Liu Y, Zhang C. Mechanical properties of La 2 O 3 doped diamond-like carbon films. Appl Surf Sci. 2008;254:7193-7197.
24. Zhou S, Wang L, Wang SC, Xue Q. Comparative study of simplex doped nc-WC/a-C and duplex doped nc-WC/a-C(Al) nanocomposite coatings. Appl Surf Sci. 2011;257:6971-6979.
25. Murata J, Ueno Y, Yodogawa K, Sugiura T. Polymer/CeO 2 –Fe 3 O 4 multicomponent core–shell particles for high-efficiency magneticfield-assisted polishing processes. International Journal of Machine Tools & Manufacture. 2016;101:28-34.
26. Wang AY, Lee KR, Ahn JP, Han JH. Structure and mechanical properties of W incorporated diamond-like carbon films prepared by a hybrid ion beam deposition technique. Carbon. 2006;44:1826-1832.
27. Modabberasl A, Kameli P, Ranjbar M, Salamati H, Ashiri R. Fabrication of DLC thin films with improved diamond-like carbon character by the application of external magnetic field. Carbon. 2015;94:485-493.
28. Cui L, Lu Z, Wang L. Probing the low-friction mechanism of diamond like carbon by varying of sliding velocity and vacuum pressure. Carbon. 2013;66:259-266.
29. Kilman L, Jaoul C, Colas M, et al. Friction and wear performance of multilayered a-C:H:Al coatings. Surface & Coatings Technology. 2015;284:159-165.
30. Du P, Chen G, Song S, Chen H, Li J, Shao Y. Tribological Properties of Muscovite, CeO2 and Their Composite Particles as Lubricant Additives, Tribology Letters, 62 (2016).
31. Andersson J, Erck RA, Erdemir A. Friction of diamond-like carbon films in different atmospheres. Wear. 2003;254:1070-1075.
32. Ronkainen H, Varjus S, Holmberg K. Tribological performance of different DLC coatings in water-lubricated conditions. Wear. 2001;249:267-271.
33. Erdemir A. Genesis of superlow friction and wear in diamondlike carbon films. Tribology International. 2004;37:1005-1012.

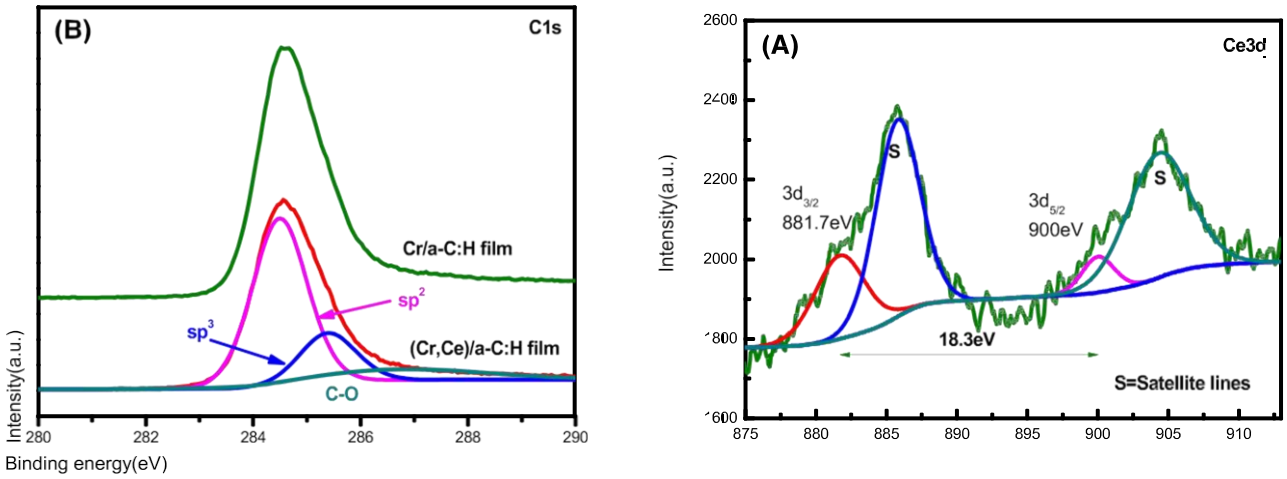

FIGURE 1 (A) X - ray photoelectron spectroscopy Ce3d spectra of (Cr, Ce)/a - C:H film and (B) X - ray photoelectron spectroscopy C1s spectra of Cr/a - C:H and (Cr,Ce)/a - C:H films

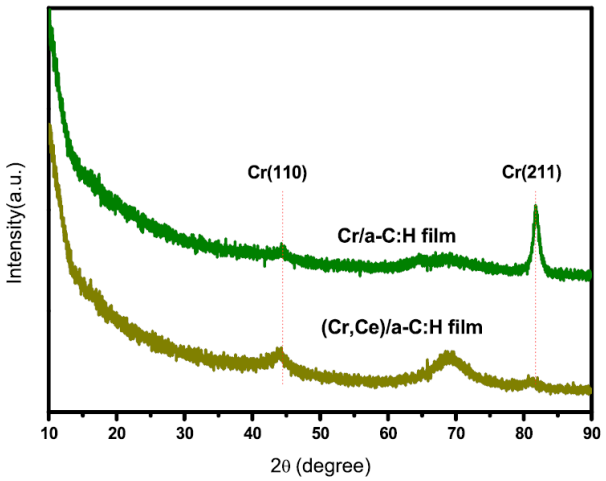

FIGURE 2 X - ray photoelectron spectroscopy spectra of as - prepared Cr/a - C:H and (Cr,Ce)/a - C:H films

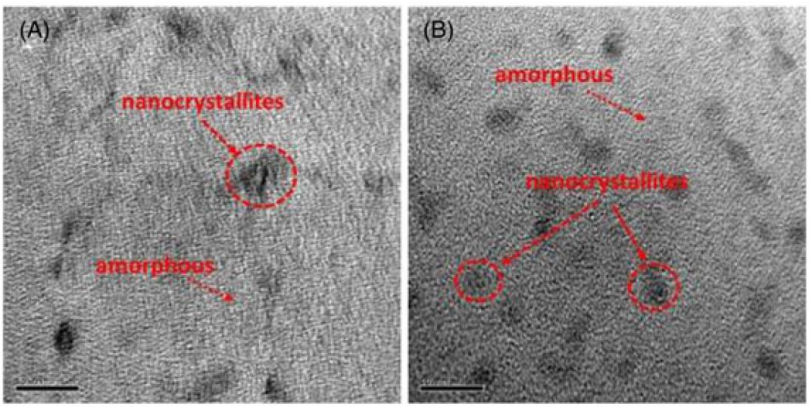

FIGURE 3 HRTEM bright - field images: (A) Cr/a - C:H film and (B) (Cr,Ce)/a - C:H film

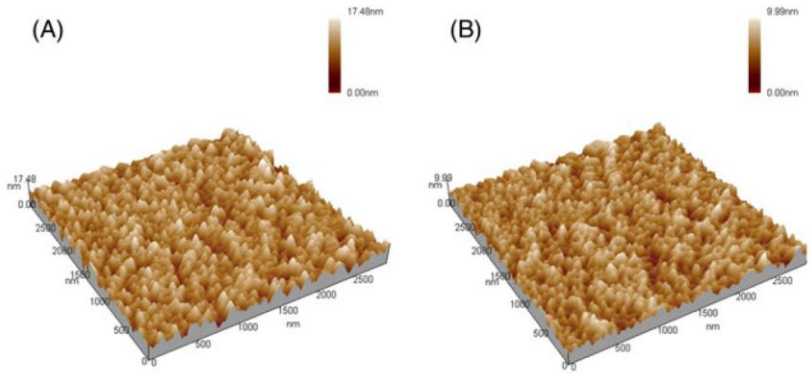

FIGURE 4 The 3‐dimensional atomic force microscopy surface morphologies: (A) Cr/a‐C:H film and (B) (Cr,Ce)/a‐C:H film

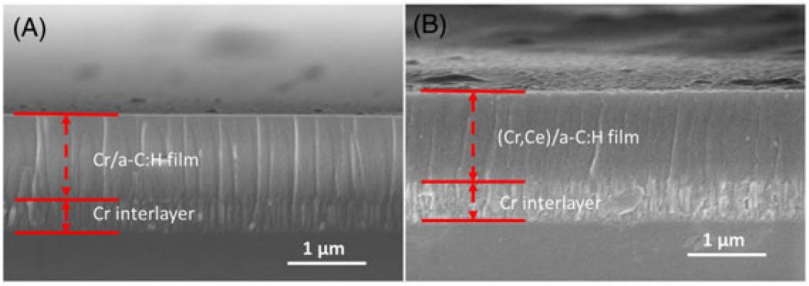

FIGURE 5 Cross‐sectional images of as‐fabricated films: (A) Cr/a‐C:H film and (B) (Cr,Ce)/a‐C:H film

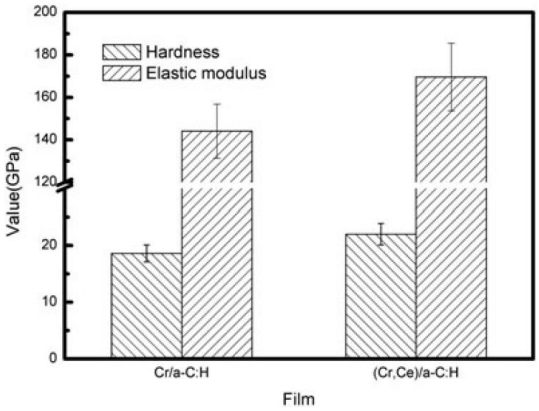

FIGURE 6 The hardness and elastic modulus of the Cr/a‐C:H and (Cr, Ce)/a‐C:H films

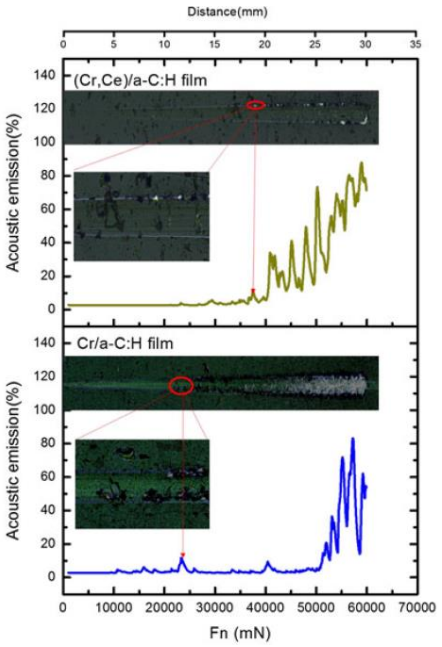

FIGURE 7 The optical microscope images and acoustic emission of scratch tests for the Cr/a‐C:H and (Cr,Ce)/a‐C:H films

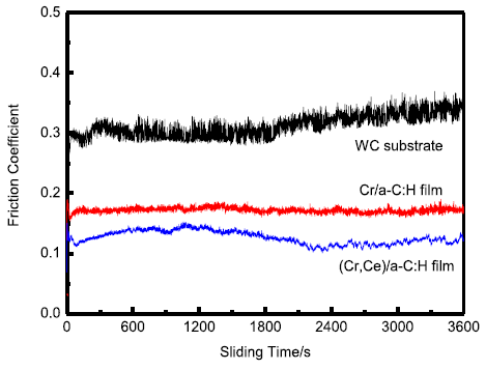

FIGURE 8 Friction coefficient versus sliding time for cemented tungsten carbide (WC) substrate, Cr/a‐C:H film, and (Cr,Ce)/a‐C:H film in ambient air

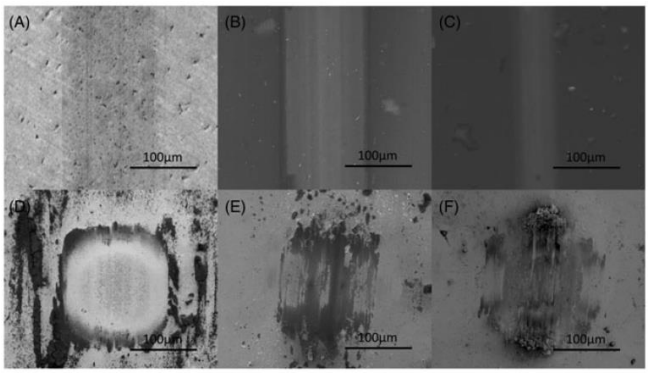

FIGURE 9 Scanning electron microscope images of wear tracks and wear scars on the counterfaces in ambient air: (A) and (D) for cemented tungsten carbide substrate; (B) and (E) for Cr/a‐C:H film; (C) and (F) for (Cr,Ce)/a‐C:H film

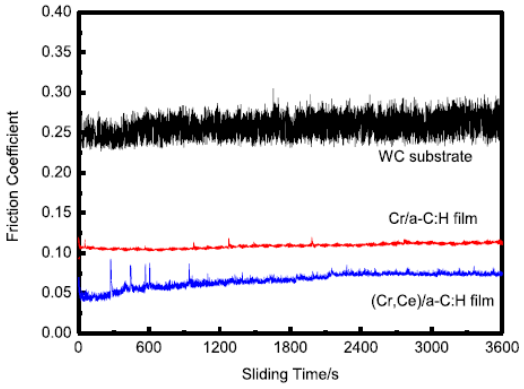

FIGURE 10 Friction coefficient versus sliding time for Cr/a‐C:H film and (Cr,Ce)/a‐C:H film in deionized water. WC, tungsten carbide

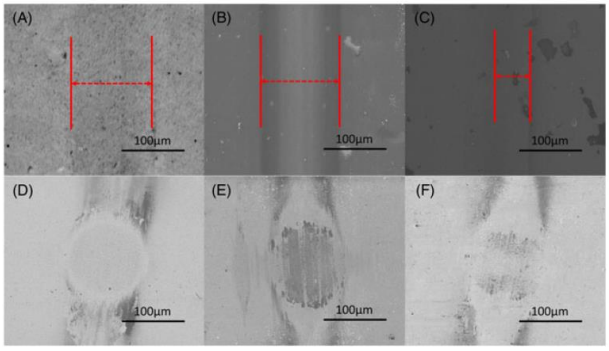

FIGURE 11 Scanning electron microscope images of wear tracks and wear scars on the counterfaces in deionized water: (A) and (D) for cemented tungsten carbide (WC) substrate; (B) and (E) for Cr/a‐C:H film; (C) and (F) for (Cr,Ce)/a‐C:H film